PROCEEDINGS OF SCIENCE

Discovery of the Ultra-High-Energy gamma-ray source LHAASO J2002+3238 spatially associated with SNR G69.7+1.0

B.W.Hou,[a,b,c,*] **R.Zhang,**[d,e] **S.Q.Xi,**[a,c] **S.Z.Chen,**[a,c] **H.N.He,**[e] **Z.Q.Xia**[e] **and LHAASO collaboration**

[a] *Key Laboratory of Particle Astrophyics & Experimental Physics Division & Computing Center, Institute of High Energy Physics, Chinese Academy of Sciences, 100049, Beijing, China*

[b] *University of Chinese Academy of Sciences, 100049, Beijing, China*

[c] *Tianfu Cosmic Ray Research Center, 610000 Chengdu, Sichuan, China*

[d] *University of Science and Technology of China, 230026, Hefei, China*

[e] *Key Laboratory of Dark Matter and Space Astronomy & Key Laboratory of Radio Astronomy, Purple Mountain Observatory, Chinese Academy of Sciences, 210023, Nanjing, China*

E-mail: houbw@ihep.ac.cn, zhangrui@pmo.ac.cn, xisq@ihep.ac.cn, chensz@ihep.ac.cn, hnhe@pmo.ac.cn, xiazq@pmo.ac.cn

The origin of Galactic PeV cosmic rays is still under debate. Shell-type supernova remnants (SNRs) are proposed to be one of the candidate sources of Galactic PeV cosmic rays, but observational evidence is lacking. Here we report LHAASO's detection on a point source J2002+3238 with a significance of 5.8 sigma above 25 TeV and 6.8 sigma above 100 TeV. The spectrum is consistent with a power-law spectrum with no cutoff. Inside the error region of the source, a shell-type SNR G69.7+1.0 is found locating only 0.07°away from the best-fit location of the source, suggesting a strong association between the UHE gamma-ray source and the SNR. This provides strong evidence on SNRs as possible PeV accelerators.

38th International Cosmic Ray Conference (ICRC2023)
26 July - 3 August, 2023
Nagoya, Japan

*Speaker

PoS(ICRC2023)605

1. INTRODUCTION

KM2A is the largest array of the large-area, high-sensitivity, wide field-of-view and wide energy-range for high-energy CRs and γ-ray air shower array, LHAASO. KM2A is the most sensitive array at VHE energy-range for now, so it finds sever new VHE sources with the significance upper than 5σ, and one of the sources is located at R.A. 300.65, Dec 32.65 named LHAASO J2002+3238, which is near the position of SNR G69.7+1.0.

The SNR G69.7+1.0 was first proposed as a supernova remnant(SNR) at radio range [11], the radio spectrum index is about -0.7 [5], and was verified by other study [4], from these works we know the position of the SNR is R.A. 300.68, Dec 32.72,and the diameter is $16'$, but different studies give different distance of the SNR to earth from 14.4 kpc to 7.8 kpc [3, 6, 9]. There is a new SNR named SNR G69.4+1.2 which its diameter is about 1° and the distance to earth is about 2.5 kpc was found surrounding the SNR G69.7+1.0, with the study of optical and X-ray emission by sever experiments [7, 8, 10]. But at the γ-ray range, only Fermi-LAT has observation at the energy lower than 10 TeV, and find a source named 4FGL J2002.3+3246 with the significance upper than 4 [1].

With the KM2A observation, we can draw a multi-wavelength research map of the SNR G69.7+1.0 region. Because there are sever stronger VHE sources in the region, the multi source simultaneous fitting is needed.

2. LHAASO-KM2A Observation

2.1 LHAASO-KM2A Detector

LHAASO-KM2A is a typical EAS array, has the characteristics of all-weather and large field of view. It can scan the sky with the earth's rotation and continuously measure EAS.It has two kind fo sub detectors which are EDs and MDs.

The EDs are mainly used to detect the electromagnetic particle information in the EAS, and can provide the number and the arrival time information of particles for the event reconstruction. Each ED contains plastic scintillator, wavelength shift optical fiber, photomultiplier tube, electronics and other devices. When the electromagnetic particles hit the scintillator, the scintillation light will be generated, collected and transmitted to the photomultiplier tube through the optical fiber, and then converted into electrical signals, which are converted into digital signals by electronics and recorded. They are arranged in a triangle with the interval of 15m within the radius of 575m and the interval of 30m between the radius of 575-635m.

The MDs are used to detect the muon in the cascade shower to identify the shower type. MD is covered under the 2.5m soil layer, which can effectively shield the electromagnetic components in the shower. The main body of the MD is a cylindrical tank with a special water bag containing ultrapure water. When the muon is incident on the water, it will generate Cherenkov light, which is received by the photomultiplier tube and converted into an electrical signal through multiple reflections of the water bag, and then converted into a digital signal by electronics and recorded. They are also arranged in a triangle with an interval of 30m.

2.2 Analysis Method

The data we use in this analysis were collected by the half array of KM2A from December 27, 2019 to December 01, 2020, the three-fourths array form December 01, 2020 to July 20, 2021, and the full array form July 20, 2021 to September 30, 2022. And the energy-range is above 25 TeV (log_{10TeV}E > 1.2).

The ED detectors in KM2A are used to recorded the arrival time and deposited energy of γ-rays, which can be used to reconstruct the direction. And the MD detectors in KM2A are used to distinguish the cosmic rays and γ-rays, using the MC events of γ-rays and the real cosmic rays data, KM2A can reject the cosmic rays background by 99% at 20 TeV and 99.99% above 100 TeV with the 90% efficiency of γ-rays maintaining. The event selection conditions we used in this work are the same like those in the work of Crab Nebula analysis before [2].

We define ρ_{50} as the particle density in the perpendicular distance of 50 m form the shower axis, use the best-fit NKG function to estimate the primary energy of the γ-rays. For showers which have the zenith angles less the 20°, using this method can have a energy resolution about 24% at 20 TeV and 13% at 100 TeV[2].

The sky map of the target source is divided into many bins with the size of 0.1° of right ascension (R.A.) and declination (Dec.). We use the so called direct integration method to estimated the background around the target source, which can estimates the background by using the events in the same direction but in different arrival times. We defined the radius of the target source as three times of the width of a Gaussian function, and that is the convolution of the point-spread function (PSF) of the KM2A and the extension of the target source. By using this method we can eliminate the effects of the instrumental and environmental variations.

We use a test statistic variable as two times of the logarithmic likelihood ratio to estimated the significance of the target source. We define L_{s+b} as the maximum likelihood for the signal and background hypothesis, and define L_b as the maximum likelihood for background only, so that TS = 2ln(L_{s+b}/L_b). As the Wilks' theorem told, in the case of background only, the value of TS is following a n degrees freedom χ^2 distribution, and n is the number of signal model free parameters. For a point source with fixed position, when we ignoring the spectral distribution of normalization, there is only one free parameter, and the pre-trial significance is $\sqrt{TS}$.

To measure the spectral energy distribution (SED) of the target source, we use a binned-likelihood forward-fording procedure. We count the number of γ-rays events in three bins with a width of Δlog_{10}E = 0.2, ranged from to. And we got the SED of the target source follow a power-law distribution, which is dN/dE = $J_0 \times (E/E_0)^{-\gamma}$, where E_0 = is the reference energy. We got the best-fit value of J_0 and γ by the maximum likelihood algorithm.

3. Result

In Figure 1 we show the significance maps around SNR G69.7+1.0 in both energy ranges of 25−100 TeV and >100 TeV, which you can see the distance of our new point *gamma*-ray source LHAASO J2002+3238 is very close to the SNR. The source is detected with a statistical significance of 4.4σ and 6.8σ, respectively. And in energy range of ≥25 TeV, we use point source model and 2D Gaussian expansion model using the maximum likelihood method to determine the most likely source model parameters for further analysis, the result is shown in Table 1.

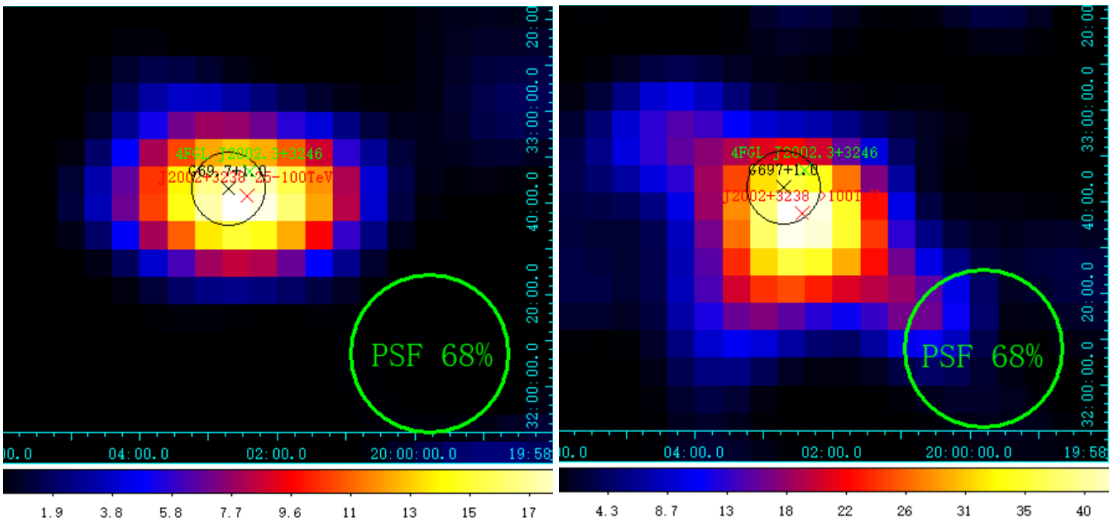

Figure 1: Left: significance map around G69.7+32.8 as observed by KM2A for reconstructed energies from 25 TeV to 100 TeV. Right: significance map for energies above 100 TeV. The black cross and circle denote the position and the size of the SNR G69.7+1.0 observed in radio energy range. The green cross denote the position of 4FGL J2002.3+3246 observed by Fermi-LAT . The red cross denote the position of LHAASO J2002+3238, and the green circle at bottom-right corner shows the size of PSF (containing 68% of the events).

Table 1: The Morphology analyses of LHAASO J2002+3238

Template	**Extension**	**RA**	**Dec**	**TS**
Pointsource	—	300.61 ± 0.05	32.64 ± 0.02	44.28
2DGaussian	0.02 ± 0.03	300.61 ± 0.09	32.64 ± 0.07	45.01

The best fitting TS value in ≥ 25 TeV energy band for the point source model is 44.28, while for the 2D Gaussian model is 45.01, comparing to the point source model, the 2D Gaussian fitting model has a significance of only 0.85 σ, which is not better enough than the point source model, so we will use the point source model to fit the source.

4. Multi-Wavelength Study and Discussions

For the SNR G69.7+1.0, there are several studies mostly under radio energy bands so far, IRAS observed the region at 4650 MHz and the Effelsberg 11 cm survey give the observation result at 2695 MHz[11], then the GCPS collaboration got a radio continuum spectra superadd their new observation result at 1420 MHz and 408 MHz[5].

A source 4FGL J2002.3+3246 observed by Fermi-LAT in this position[12]. As for the Fermi-LAT observation, we select more than 14 years LAT Pass8 (P8R3, the latest version) data from October 27, 2008, to March 14, 2023 with energies from 300MeV to 1 TeV within the $14^\circ \times 14^\circ$ region of interest (ROI) centered on the target 4FGL J2002.3+3246. Here we use the binned likelihood method to do the overall fitting and calculate the spectral energy distribution (SED). We take the spectral shape of 4FGL J2002.3+3246 as the Power-Law function which is the same as in the fourth Fermi-LAT source catalog (4FGL). In the overall fitting, normalizations of the galactic and isotropic diffuse models are considered to be free parameters. Moreover, normalizations and spectral indices of all the 4FGL sources within 5° from the target are also set to be free. We obtain the TS value of 4FGL J2002.3+3246 is 65.5 with the best-fit index 2.73. To calculate the SED, we divide events into 7 evenly spaced logarithmic energy bins from 300 MeV to 1 TeV. Here the spectral indices of all sources are fixed as the best-fit value from the overall fitting, while their normalizations are leave to be free. Then we repeat the binned likelihood analysis in each energy bins. The `UpperLimits` tool in the `Fermitools` package is used to calculate the 95% upper limit of the flux in the energy bin where the TS value is smaller than 9. The Fermi-LAT SED is marked in red in the Fig. 2.

Other experiments also have observed this region in the gamma range, a job deep observations toward the Cygnus region using 300 hr of very high energy (VHE) γ-ray data taken with the VERITAS Cerenkov telescope array gives a upper limit of this source [14] and H.E.S.S. also give a upper limit to this SNR [15]. In addition, LHAASO-WCDA has also observed phenomena here, but its significance has not yet reached 5 σ.

The radio observations can be fit by the synchrotron emission of non-thermal electrons. The GeV observations by Fermi-LAT can be explained by the bremsstrahlung emission of electrons. The $>$ 25 TeV photons observed by the LHAASO KM2A can be produced by either the inverse Compton emission of electrons scattering the CMB photons, or the proton-proton collision between the accelerated protons interact with the medium. The energy distributions of electrons and protons are assumed to follow the exponential cutoff power-law function. The contributions from the leptonic components and hadronic components are calculated via adopting the software Naima [13]. The pure leptonic scenario is plotted in Figure 2. The total energy of injected electrons is required to be 1.6×10^{48}erg by assuming the distance of the supernova is 7.8 kpc. The hybrid scenario is plotted in Figure 3. The total energy of injected electrons is 8.5×10^{47}erg and the total required energy of injected protons is 1.5×10^{48}erg. To produce $>$ 25TeV photons via inverse Compton emission of electrons, electrons need to be accelerated to the energy as high as 150 TeV, leading to a high fluence in the keV band. Thus, the X-ray observation on this source can further constrain the model. What's more, our future study adopting multi-wavelength observations will help us to constrain the age, the distance and the environment of the supernova, and further help us to distinguish between the leptonic model and the hybrid model.

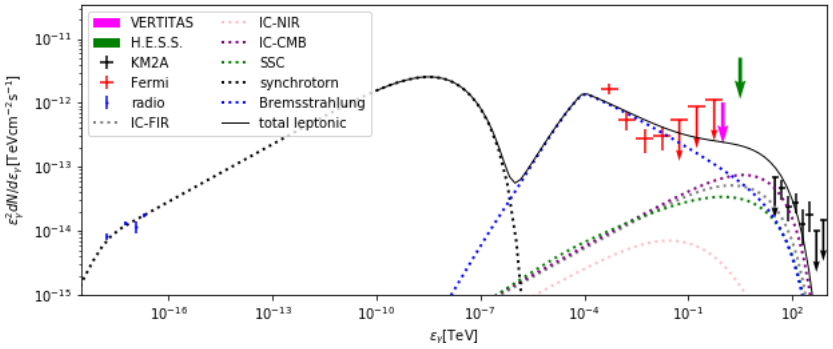

Figure 2: The multi-wavelength spectrum in the leptonic scenario. The blue data is the radio observations, the red data is the Fermi-LAT observations, and the black data is the LHAASO KM2A observation. The injected spectrum of electrons is assumed to be $\frac{dN_e}{d\varepsilon_e} \propto \varepsilon_e^{-2.4}\exp[-(\varepsilon_e/120\mathrm{TeV})]$, with the lowest energy of electrons as $\varepsilon_{e,\mathrm{min}} = 0.1\mathrm{GeV}$. The strength of magnetic field is assumed to be $B = 15\mu\mathrm{G}$, the number density of the medium is assumed to be $n_\mathrm{H} = 40\mathrm{cm}^{-3}$ and the distance of the supernova is $D_\mathrm{L} = 7.8\mathrm{kpc}$.

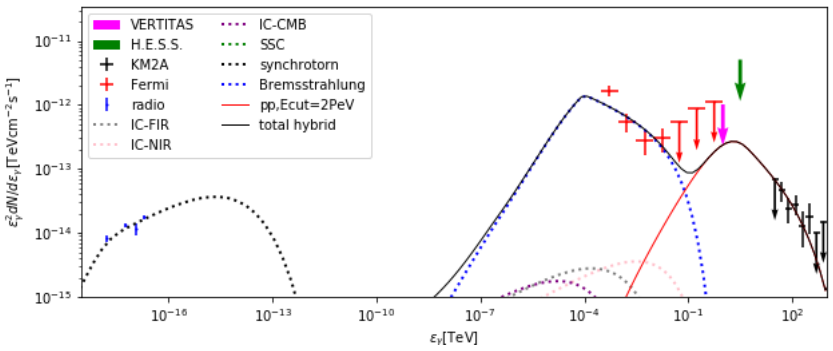

Figure 3: The multi-wavelength spectrum in the hybrid scenario. The blue data is the same as in Fig 2.The injected spectrum of electrons is assumed to be $\frac{dN_e}{d\varepsilon_e} \propto \varepsilon_e^{-2.4}\exp[-(\varepsilon_e/0.1\mathrm{TeV})]$, with the lowest energy of electrons as $\varepsilon_{e,\mathrm{min}} = 0.1\mathrm{GeV}$.The injected spectrum of protons is assumed to be $\frac{dN_p}{d\varepsilon_p} \propto \varepsilon_p^{-2.6}\exp[-(\varepsilon_p/2\mathrm{PeV})]$, with the lowest energy of protons as $\varepsilon_{p,\mathrm{min}} = 8\mathrm{TeV}$.The strength of magnetic field, the number density of the medium and the distance of the supernova adopted are the same as in Fig 2.

References

[1] Abdollahi, S., Acero, F., Baldini, L., et al. 2022, ApJ, 260, 53. doi:10.3847/1538-4365/ac6751

[2] Aharonian, F., An, Q., Axikegu, et al. 2021, Chinese Physics C, 45, 025002. doi:10.1088/1674-1137/abd01b

[3] Pavlović, M. Z., Urošević, D., Vukotić, B., et al. 2013, ApJS, 204, 4. doi:10.1088/0067-0049/204/1/4

[4] Sun, X. H., Reich, P., Reich, W., et al. 2011, AAp, 536, A83. doi:10.1051/0004-6361/201117693

[5] Kothes, R., Fedotov, K., Foster, T. J., et al. 2006, AAp, 457, 1081. doi:10.1051/0004-6361:20065062

[6] Guseinov, O. H., Ankay, A., & Tagieva, S. O. 2003, Serbian Astronomical Journal, 167, 93

[7] Mavromatakis, F., Boumis, P., & Paleologou, E. V. 2002, AAp, 387, 635. doi:10.1051/0004-6361:20020398

[8] Yoshita, K., Miyata, E., & Tsunemi, H. 2000, PASJ, 52, 867. doi:10.1093/pasj/52.5.867

[9] Case, G. L. & Bhattacharya, D. 1998, ApJ, 504, 761. doi:10.1086/306089

[10] Asaoka, I., Egger, R., & Aschenbach, B. 1996, Roentgenstrahlung from the Universe, 233

[11] Junkes, N., Fürst, E., & Reich, W. 1988, Supernova Shells and Their Birth Events, 134. doi:10.1007/3-540-50435-4_18

[12] Ajello, M., Angioni, R., Axelsson, M., et al. 2020, ApJ, 892, 105. doi:10.3847/1538-4357/ab791e

[13] Zabalza, V. 2015, 34th International Cosmic Ray Conference (ICRC2015), 34, 922. doi:10.22323/1.236.0922

[14] Abeysekara, A. U., Archer, A., Aune, T., et al. 2018, ApJ, 861, 134. doi:10.3847/1538-4357/aac4a2

[15] H. E. S. S. Collaboration, Abdalla, H., Abramowski, A., et al. 2018, AAp, 612, A3. doi:10.1051/0004-6361/201732125